An innovative energy management framework for cooperative operation management of electricity and natural gas demands

N. Gholizadeh[a], G. B. Gharehpetian[a], M. Abedi[a], H. Nafisi[a], M. Marzband[b,*]

[a]*Department of Electrical Engineering, Amirkabir University of Technology (Tehran Polytechnic), Tehran, Iran*
[b]*Department of Mathematics, Physics and Electrical Engineering, Northumbria University, Newcastle, UK*

Abstract

Introduction of the power to gas and combined heat and power technologies, has led to remarkable interdependency between electrical and gas systems. By taking advantage of this interdependency, cleaner and more efficient energy management systems could be implemented. This paper attempts to establish an innovative energy management framework which takes advantage of this interdependency and devices like power to gas and combined heat and power to simultaneously smoothen electricity and natural gas demand profiles for a year ahead. The method outperforms this task using the electricity profile valleys to reduce peak natural gas consumption and using natural gas profile valleys to shave electricity consumption peak. In this way, the stress on both networks for supplying demand in peak periods is released. The proposed method is able to achieve demand smoothness and cost reduction objectives considering penalty factors for demand variance. For this purpose, multiple integrated energy hubs are used to simulate the energy consumption of an area. The designed mixed integer linear model is handled by General Algebraic Modeling Software and CPLEX solver. The results demonstrate that by applying the proposed method, the system is able to save 16.92% in the energy cost and decrease electricity and natural gas demand standard deviations by 8.34% and 66.64%, respectively.

Keywords: Combined heat and power, Electricity and natural gas scheduling, Energy hubs,

*Corresponding author.
Email address: mousa.marzband@northumbria.ac.uk (M. Marzband)

Load smoothing, Peak shaving, Power to gas technology

Nomenclature

General indices

j	Auxiliary index as an alternative for hub counter
le	Index indicating the number of electrical grids
lg	Index indicating the number of gas grids
n	Index showing hub counter
t	Index showing time [hr]

Parameters

α	Smoothness coefficient
η^{Echp}/η^{Tchp}	Efficiency of electrical/thermal energy production by CHP [%]
η^{ES+}/η^{ES-}	Charging/discharging efficiency for electrical storage [%]
η^{e}/η^{m}	Efficiency of electrolyzer unit/methanization process [%]
η^{HS+}/η^{HS-}	Charging/discharging efficiency for hydrogen storage [%]
η^{tr}/η^{gb}	Efficiency of transformer/gas boiler [%]
η^{TS+}/η^{TS-}	Charging/discharging efficiency for thermal storage [%]
μ^{e}/μ^{g}	Mean of electricity/natural gas demand [kW]
$\overline{\alpha}^{ES}/\underline{\alpha}^{ES}$	Maximum/minimum level ratio for electrical storage

$\overline{\alpha}^{HS}/\underline{\alpha}^{HS}$	Maximum/minimum level ratio for hydrogen storage
$\overline{\alpha}^{TS}/\underline{\alpha}^{TS}$	Maximum/minimum level ratio for thermal storage
$\overline{P}^{ES+}/\overline{P}^{ES-}$	Maximum charging/discharging rate of electrical storage [kW]
$\overline{P}^{ex}$	Maximum electrical power hubs can exchange [kW]
$\overline{P}^{HS+}/\overline{P}^{HS-}$	Maximum charging/discharging rate of hydrogen storage [kW]
$\overline{P}^{tr}/\overline{P}^{chp}/\overline{P}^{gb}$	Maximum power input of transformer/CHP/gas boiler [kW]
$\overline{P}^{TS+}/\overline{P}^{TS-}$	Maximum charging/discharging rate of thermal storage [kW]
$\overline{v}/\underline{v}$	Maximum/minimum wind speed of wind turbine [m/s]
π^{ep}/π^{gp}	Penalty costs for per unit of variance in electricity/natural gas demand [¢/(kWh)^2]
π_t^e/π^g	Electricity/natural gas prices [¢/kWh]
$C^{ES}/C^{HS}/C^{TS}$	Capacity of electrical/hydrogen/thermal storage [kWh]
$I_{le,n}^{hg}/I_{lg,n}^{he}$	Binary parameters showing electrical/gas grids each hub is fed from
I_{le}^{p}/I_{le}^{w}	Binary parameters representing the connection nodes of P2G/wind turbine
$I_{n,j}^{ec}$	Binary parameter showing connection state of hubs for electricity exchange
$L_{t,n}^{e}/L_{t,n}^{t}$	Electrical/thermal loads [kW]
P^r	Wind turbine rated power [kW]
P_t^{WT}	Electrical power generated by wind turbine [kW]

60 v^r Wind turbine rated speed [m/s]

61 v_t Wind speed [m/s]

62 ***Variables***

63 $E_{t,n}^{ES}/E_{t,n}^{HS}/E_{t,n}^{TS}$ Electrical/hydrogen/thermal storage level [kWh]

64 $I_{t,n}^{ES+}/I_{t,n}^{ES-}$ Binary variables showing charging/discharging status of electrical storage

65 $I_{t,n}^{HS+}/I_{t,n}^{HS-}$ Binary variables showing charging/discharging status of hydrogen storage

66 $I_{t,n}^{TS+}/I_{t,n}^{TS-}$ Binary variables showing charging/discharging status of thermal storage

67 P_t^m Total produced methane power from methanization process [kW]

68 $P_{t,le}^{Enet}$ Electrical power imported from each electrical grid [kW]

69 $P_{t,lg}^{H}/P_{t,lg}^{pipe}$ Injected hydrogen/methane power into each gas pipeline [kW]

70 $P_{t,lg}^{Gnet}$ Natural gas power imported from each gas pipeline [kW]

71 $P_{t,n,j}^{ex}$ Exchanged electrical power between hubs [kW]

72 $P_{t,n}^{e}/P_{t,n}^{g}$ Electricity/natural gas input of each hub [kW]

73 $P_{t,n}^{chp}/P_{t,n}^{gb}$ Natural gas input of CHP/gas boiler [kW]

74 $P_{t,n}^{ES+}/P_{t,n}^{ES-}$ Charging/discharging power of electrical storage [kW]

75 $P_{t,n}^{HS+}/P_{t,n}^{HS-}$ Charging/discharging power of hydrogen storage [kW]

76 $P_{t,n}^{TS+}/P_{t,n}^{TS-}$ Charging/discharging power of thermal storage [kW]

77 P_t^c Curtailed wind turbine power [kW]

$P_t^{ptg}/P_{t,n}^{tr}$ Electricity input of electrolyzer/transformer [kW]

1. Introduction

The increasing interactions between electrical and gas systems has led to development of affordable and cleaner energy systems. This has been achieved by introducing the energy hub concept [1], which is an interface among different energy vectors and contains devices such as power to gas systems (P2G), combined heat and power systems (CHP), electric boilers and etc. [2]. Designing a proper energy management structure for these energy hubs can bring many benefits for consumers and environment such as cost and CO2 reduction [3]. Recently, there has been a widespread investigation about the P2G systems in literature. The process simply includes conversion of electrical energy to hydrogen or methane via electrolysis and methanization methods, respectively [4]. The produced gas can be stored or directly used to generate electricity or heat [5].

The P2G technology has been used for various purposes in literature. For example, Maroufmashat et al. in [6] have optimized the cost of managing energy in future communities by using hydrogen as an energy vector. They have also determined the optimal size of the electrolyzer and hydrogen storage system used inside the P2G unit. Chen et al. in [7] have studied the effect of uncertainties of both electrical and gas systems on overall operating states of integrated energy systems. It has been found that P2G benefits electrical and gas grids in several ways including curtailment and congestion relief in electricity network, reinforcement of gas network and etc. Authors of [8] and [9] have studied the role of energy storage in P2G systems. However, Ni et al. in [8] have considered roles of different types of energy storage systems inside an energy hub containing P2G unit, while in [9], Walker et al. have compared P2G with other storage technologies in different applications

using Analytical Hierarchy Process. The authors have found that considering criteria such as portability, energy density and ability for seasonal storage make P2G very useful in utility scale energy storage applications. Also, Al Rafea et al. have investigated the integration of renewable energy resources into larger scale fossil fueled combined cycle power plants by considering hydrogen as an energy vector [10]. It has been shown that using hydrogen as a fuel in combined cycle power plants would create extra cost and decrease annual revenues. In [11], Gholizadeh et al. have used P2G to decrease the amount of electrical and thermal load shedding in case of electricity and gas network contingencies. In [12], Antenucci et al. have optimized the placement of P2G stations within the electrical network to allow complete recycling of CO2 emissions of electric power system. Qu et al. in [13] have proposed a novel robust multi-objective power and gas flow for power and natural gas coupled systems utilizing P2G systems. Three objectives have been defined for the system under study: minimization of energy supply cost, minimization of carbon emissions and smoothing of net power demand. He et al. have designed a two-stage and day-ahead scheduling framework of the power and gas systems while ensuring security of the both systems [14]. The utilization of the P2G has been presented in [15] as an energy balancing system in wind farms to assess its economic, energy and environmental effects and in [16], different transformation technologies, distribution options, geological storage options and end user applications of the P2G system have been presented. Also, Vandewalle et al. have investigated the impact of P2G on gas, electricity and CO2 sector and its effect on the interaction between these sectors and have shown that P2G partially transfers uncertainties in the electricity sector to the gas sector [17].

Extensive research on CHP units has been carried out in literature. Many studies have

used CHP to decrease power system operation costs [18], while some studies have used it for purposes like pollution reduction [19], system's operational efficiency improvement [20], increasing productivity of solar cells [21], increasing decentralized energy supply [22], improving system reliability [23], power peak shaving [24] and etc.

In order to maintain power system stability, electrical loads need to be fulfilled in all times [25]. This is a big challenge to electric utility in peak consumption periods especially with rapid development of industrialization [26]. As the weather changes during a year, electrical and gas demands change accordingly. For the cities, like Philadelphia, which rely on natural gas to provide their thermal loads, the electricity usage falls in cold seasons while the natural gas needs rise. On the other hand, during the warmer seasons, the electricity demand increases while natural gas loads decrease. Since these two energy types are among the most important and highly used energy carriers in urban areas, smoothing both load curves and shaving peak load will release the stress on the energy system for maintaining energy balance and will allow better utilization of generation capacity of power plants and energy resources [27]. Moreover, this will prevent leveraging of power plants (i.e., installing new power plants) for supplying small rises in consumption during peak. Many strategies have been proposed in literature to shave the peak load of electrical systems. They include using battery energy storage systems (BESSs) [28], plug-in hybrid electric vehicles (PHEVs) [29], demand side management (DSM) techniques [30], pumped storage power plants (PSPPs) [31] and etc. The peak shaving will increase load factor and system efficiency [32], enhance power quality and reliability, and finally reduce cost and carbon emission [33]. A limited number of recent studies have focused on thermal demand peak shaving using new thermal storage technologies which store the energy in three forms: sensible heat, latent heat and thermochemical

energy storage. Studies have used hydronic floor heating system [34], electrically heated floor system [35], phase change materials [36], forced ventilation system [37] in conjunction with these storage types to shave the thermal demand peak of houses. However, no previous study has focused on simultaneous peak shaving and profile smoothing of electricity and natural gas demands. These types of multidisciplinary design optimization methods are effective in saving costs [38], improving system performance [39], enhancing safety and environmental impacts [40].

In this paper, simultaneous smoothing of electrical and natural gas demand profiles is performed by using the P2G and CHP technologies. It is shown that by taking advantage of the seasonal load changes, excess electrical energy can be converted to natural gas in colder seasons using P2G, and CHP can be used to convert natural gas to electricity during warmer seasons, which have higher electricity consumption. The contributions of this paper can be summarized as follows:

- Presenting an innovative electricity and gas profile smoothing (EGPS) method for simultaneous peak shaving and valley filling of electricity and natural gas profiles,
- Maintaining the tradeoff between energy cost saving and demand smoothing by using the proposed EGPS method,
- Determining the share of P2G, CHP and electrical storage in reducing system costs and smoothing demand profiles.

The remainder of the paper is organized in the following order. Sections (2) and (3) discuss the proposed energy hub and P2G models of this paper, respectively. Section (4) describes problem formulation. The simulation data and case studies are presented in Section

(5). The simulation results are discussed in Section (6) and finally, the concluding remarks are drawn in Section (7).

2. Energy hub model

The proposed hub model for this study is shown in Fig. 1. It can be seen that the hub receives only electricity and natural gas at the input port and fulfills electrical and thermal loads. The transformer unit inside the hub is only used for changing the voltage level. The CHP unit makes the integration of electricity and natural gas practical by using natural gas and producing both electricity and thermal energy. The gas boiler unit is only able to produce thermal energy by using natural gas. Also, the hub includes both electrical and thermal storage units.

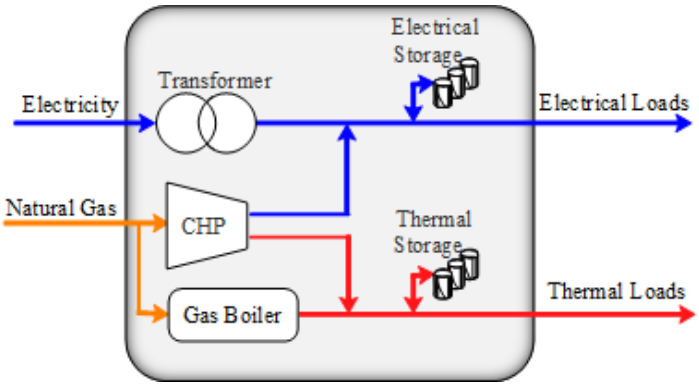

Fig. 1. Proposed energy hub model.

3. P2G model

Fig. 2 illustrates the model of the P2G unit used in this study. As shown in this figure, P2G consists of an electrolyzer that uses electricity and water to produce hydrogen. The produced hydrogen can whether be stored in the hydrogen storage tank or it can go under the methanization process that uses hydrogen and CO2 to produce methane and water. Also,

the produced hydrogen can be directly injected to the gas pipelines. However, gas pipelines become embrittled in contact with hydrogen and this limits the share of direct hydrogen injection to only 5% of total available gas energy in pipelines [41]. The electrolysis and methanization processes are modeled by their equivalent efficiency values similar to [7, 42]. The typical conversion efficiency for electrolysis process alone is 54-77% and it ranges between 49-65% for electrolysis and methanization processes together [7]. Eq. (1) models the methane injection into different gas pipelines and Eq. (2) limits the amount of direct hydrogen injection into them. The limit of the hydrogen injection is chosen to be 1% of the total natural gas energy in each pipeline in this study [11].

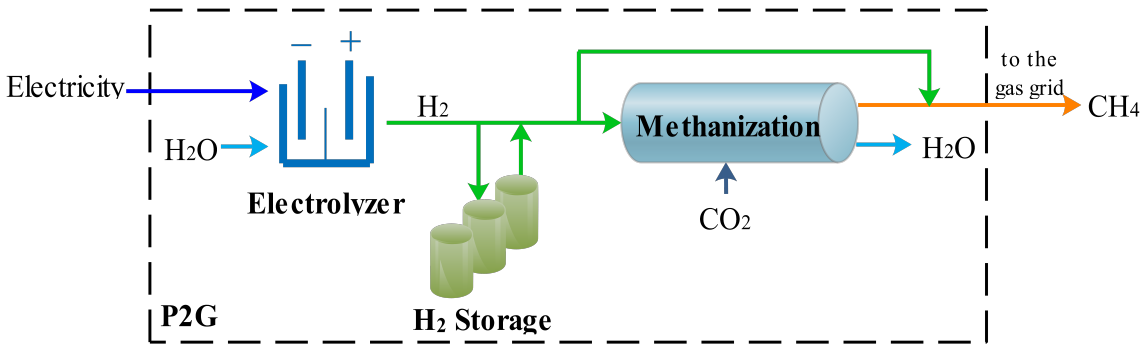

Fig. 2. P2G operation model.

$$P_t^m = \sum_{lg} P_{t,lg}^{pipe} \tag{1}$$

$$0 \leq P_{t,lg}^H \leq 0.01[P_{t,lg}^H + P_{t,lg}^{Gnet} + P_{t,lg}^{pipe}] \tag{2}$$

4. Problem formulation

Following subsections present the proposed formulation for modeling of the overall integrated hub system to apply proposed EGPS method.

4.1. Objective function

The objective function of this study is defined as Eq. (3). It consists of the total consumed electricity and natural gas cost plus the penalty considered for variances of electricity and natural gas demand profiles. The costs are summed over the whole year to obtain overall expenses.

$$OF = Cost^{energy} + \alpha Cost^{penalty} \tag{3}$$

where, we have:

$$Cost^{energy} = \sum_{t}[\sum_{le} \pi_t^e P_{t,le}^{Enet} + \sum_{lg} \pi^g P_{t,lg}^{Gnet}] \tag{4}$$

$$Cost^{penalty} = \sum_{t}[\pi^{ep}(\sum_{le} P_{t,le}^{Enet} - \mu^e)^2 + \pi^{gp}(\sum_{lg} P_{t,lg}^{Gnet} - \mu^g)^2] \tag{5}$$

The parameter α is defined here as the smoothness coefficient to control the amount of the system penalty cost and demand profile smoothness. $Cost^{energy}$ and $Cost^{penalty}$ show the total consumed energy cost and penalty cost for unsmooth demand profiles, respectively. $Cost^{energy}$ is simply obtained by multiplying the per kWh energy price in the consumed electrical and natural gas energy as defined by Eq. (4). To calculate $Cost^{penalty}$, as shown by Eq. (5), the coefficients π^{ep} and π^{gp} are used to convert the variances of electricity and natural gas demands to cost. These coefficients show the penalty cost for per unit of variance in electricity and natural gas profiles from the mean demand. In order to simplify the optimization model and ensure the global optimal operation point, the penalty costs are approximated as piecewise linear functions similar to [43].

4.2. Constraints

The set of the constraints defined for the current optimization problem, are presented in the following subsections.

4.2.1. Energy balance

In the context of energy hubs, the first and most important constraint is the energy balance constraint. It ensures that all of the system loads are met in each time step. The constraint is defined for both electrical and thermal loads by Eqs. (6) and (7), respectively.

$$L^{e}_{t,n} = \eta^{tr} P^{tr}_{t,n} + \eta^{Echp} P^{chp}_{t,n} - \eta^{ES+} P^{ES+}_{t,n} + \eta^{ES-} P^{ES-}_{t,n} + \sum_{j} P^{ex}_{t,n,j} I^{ec}_{n,j} \tag{6}$$

$$L^{t}_{t,n} = \eta^{Tchp} P^{chp}_{t,n} + \eta^{gb} P^{gb}_{t,n} - \eta^{TS+} P^{TS+}_{t,n} + \eta^{TS-} P^{TS-}_{t,n} \tag{7}$$

It is assumed that the energy hubs can exchange electrical power if they are connected to each other at the output port. The state of connectivity among hubs is shown by the parameter named $I^{ec}_{n,j}$. This parameter also models the energy losses for power exchange between hubs. As it can be seen from Eq. (6), the sum of electricity from transformer, CHP unit, electric storage and electrical energy imported from other hubs should be equal to the electrical load. Also, as stated by Eq. (7), the sum of the produced thermal energy by the CHP unit, gas boiler and heat from thermal storage should be equal to the thermal load.

Eq. (8) shows the energy balance between the imported electricity into each hub and the electricity used by devices inside that hub which is only the transformer in this study. Eq. (9) represents the same balance for natural gas. The devices which use natural gas inside each hub are CHP and gas boiler.

$$P^{e}_{t,n} = P^{tr}_{t,n} \tag{8}$$

$$P^{g}_{t,n} = P^{chp}_{t,n} + P^{gb}_{t,n} \tag{9}$$

As previously mentioned, three different storage types are used in this study. Eq. (10) determines the energy level inside each of electrical, thermal and hydrogen storages at each time step. For the sake of brevity, equations that are identical for different devices are integrated into a single equation throughout this paper.

$$E^{B}_{t,n} = E^{B}_{t-1,n} + \eta^{B+} P^{B+}_{t,n} - \frac{P^{B-}_{t,n}}{\eta^{B-}} \qquad B \in \{ES, TS, HS\} \tag{10}$$

4.2.2. Technical constraints

The technical constraints determine the size of components used inside the hubs by limiting their power input. Eq. (11) defines an upper limit for transformer, CHP and gas boiler power input.

$$0 \leq P^{D}_{t,n} \leq \overline{P}^{D} \qquad D \in \{tr, chp, gb\} \tag{11}$$

Eq. (12) specifies the maximum capacity of the electrical lines connecting the hubs. It should be noted that the electrical energy sent to other hubs is presented by a negative value for $P^{ex}_{t,n,j}$ because, it is considered as an electrical load for that hub.

$$-\overline{P}^{ex} \leq P^{ex}_{t,n,j} \leq \overline{P}^{ex} \tag{12}$$

Eq. (13) specifies the maximum and minimum allowable energy storage levels of electrical, thermal and hydrogen storages.

$$\underline{\alpha}^{B} C^{B} \leq E^{B}_{t,n} \leq \overline{\alpha}^{B} C^{B} \qquad B \in \{ES, TS, HS\} \tag{13}$$

Eq. (14) limits the maximum allowable charging rate of each of the electrical, thermal and hydrogen storages.

$$0 \leq P_{t,n}^{B+} \leq \overline{P}^{B+} I_{t,n}^{B+} \qquad B \in \{ES, TS, HS\} \tag{14}$$

The maximum discharging rates of the aforementioned three storage technologies are shown by Eq. (15).

$$0 \leq P_{t,n}^{B-} \leq \overline{P}^{B-} I_{t,n}^{B-} \qquad B \in \{ES, TS, HS\} \tag{15}$$

To prevent simultaneous charging and discharging of each storage, Eq. (16) is introduced to the each storage model.

$$0 \leq I_{t,n}^{B+} + I_{t,n}^{B-} \leq 1 \qquad B \in \{ES, TS, HS\} \tag{16}$$

4.2.3. Wind farm constraints

The power generated by the wind turbine is modeled using Eq. (17), similar to [44]. This equation shows that the generated power by the wind turbine is calculated as a function of wind speed.

$$P_t^{WT} = \begin{cases} 0 & \text{if } v_t \leq \underline{v} \text{ or } v_t \geq \overline{v} \\ \frac{v_t - \underline{v}}{v^r - \underline{v}} P^r & \text{if } \underline{v} \leq v_t \leq v^r \\ P^r & \text{if } v^r \leq v_t \leq \overline{v} \end{cases} \tag{17}$$

The wind turbine generates no electricity if the wind speed is below or over a certain value named $\underline{v}$ and $\overline{v}$, respectively. The generated electricity is linearly proportional to the wind

speed when the speed is between the rated, v^r, and the minimum wind speed. Also, the wind turbine generates a constant electricity power, P^r, when the wind speed is between the rated and the maximum value.

4.2.4. Integration of P2G and wind turbine into network

In order to integrate the wind turbine and P2G into the network, Eqs. (18) and (19) are used. Eq. (18) represents the wind turbine and P2G impact on the electrical network. Also, Eq. (19) is introduced to model the methane injection of the P2G unit to the gas network.

$$P_{t,le}^{Enet} + [P_t^{WT} - P_t^c]I_{le}^w - P_t^{ptg}I_{le}^p = \sum_n \{I_{le,n}^{hg} P_{t,n}^e\} \tag{18}$$

$$P_{t,lg}^{Gnet} + P_{t,lg}^{pipe} + P_{t,lg}^H = \sum_n \{I_{lg,n}^{he} P_{t,n}^g\} \tag{19}$$

5. Case study

The proposed formulation and strategy are applied to a network of 10 residential energy hubs. The network is shown in Fig. 3. Moreover to energy hubs, the system consists of two electrical and gas grids, a wind farm and a unit of P2G. As indicated in the figure, each hub is fed from one of the electrical and gas grids. Also, It is assumed that hubs 1 to 6 and hubs 7 to 10 are electrically connected to each other and can exchange electricity.

The basic electricity and natural gas demand data of a single house in Philadelphia area is used in this paper [45]. The energy demand of different hubs is constructed using this data considering a normal distribution function with 10% standard deviation [2]. It is assumed that each hub has 30 houses. The overall electricity and natural gas demand profiles of the system are shown in Figs. 4a and 4b, respectively. The parameters are given in Table 1 and the electricity and natural gas price data is obtained from [46, 47]. The simulation runs hourly

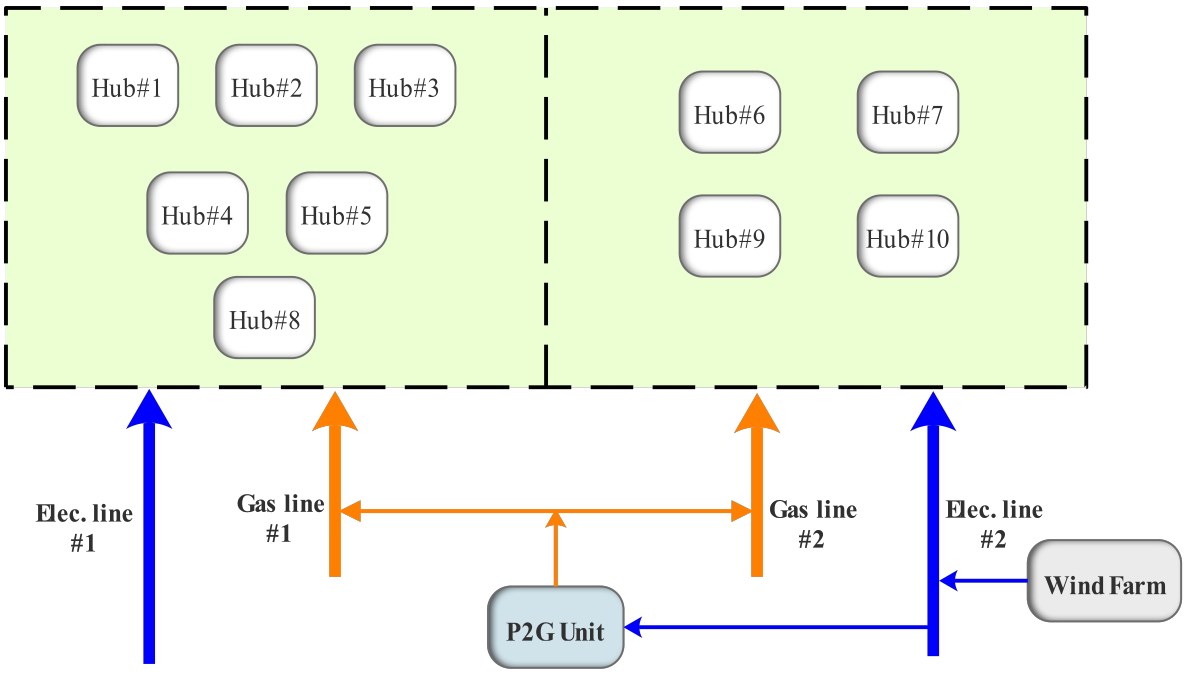

Fig. 3. System under study.

for one year period. Also, the power generated by the wind turbine is illustrated in Fig. 5.

Table 1: Parameter values.

Parameter	Unit	Amount	Parameter	Unit	Amount	Parameter	Unit	Amount
α	-	0.8	η^{ES+}, η^{ES-}	-	0.9	$\underline{\alpha}^{H}$	-	0.05
π^{ep}	cent/(kWh)^2	0.01917	η^{TS+}, η^{TS-}	-	0.9	$\overline{P}^{ES+}, \overline{P}^{ES-}$	kW	250
π^{gp}	cent/(kWh)^2	0.00556	η^{HS+}, η^{HS-}	-	0.95	$\overline{P}^{TS+}, \overline{P}^{TS-}$	kW	250
η^{tr}	-	0.95	C^{ES}	kWh	500	$\overline{P}^{HS+}, \overline{P}^{HS-}$	kW	300
η^{gb}	-	0.8	C^{TS}	kWh	400	$\overline{P}^{ex}$	kW	300
η^{Echp}	-	0.35	C^{HS}	kWh	1000	$\overline{v}$	m/s	22
η^{Tchp}	-	0.4	$\overline{\alpha}^{E}, \overline{\alpha}^{T}$	-	0.9	v_r	m/s	10
η^{m}	-	0.85	$\underline{\alpha}^{E}, \underline{\alpha}^{T}$	-	0.05	$\underline{v}$	m/s	4
η^{e}	-	0.7	$\overline{\alpha}^{H}$	-	0.95	P^r	kW	400

To show the impact of P2G, CHP and electrical storage on smoothing of electricity and natural gas demand profiles, three case studies are defined as below:

✓Case 1: EGPS method without utilizing P2G unit.

✓Case 2: EGPS method without utilizing CHP unit.

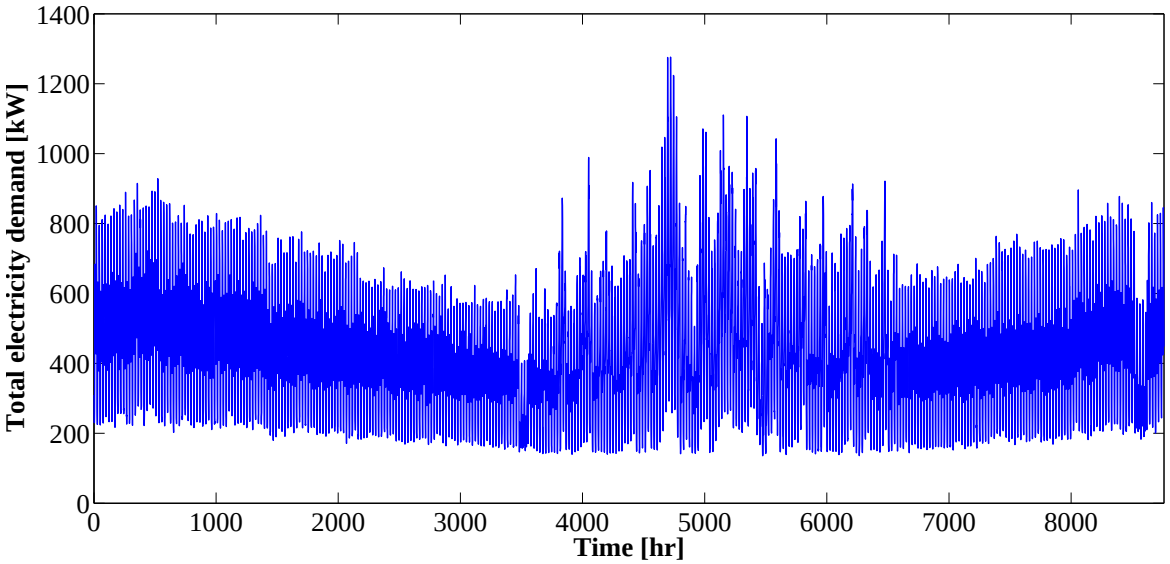

(a)

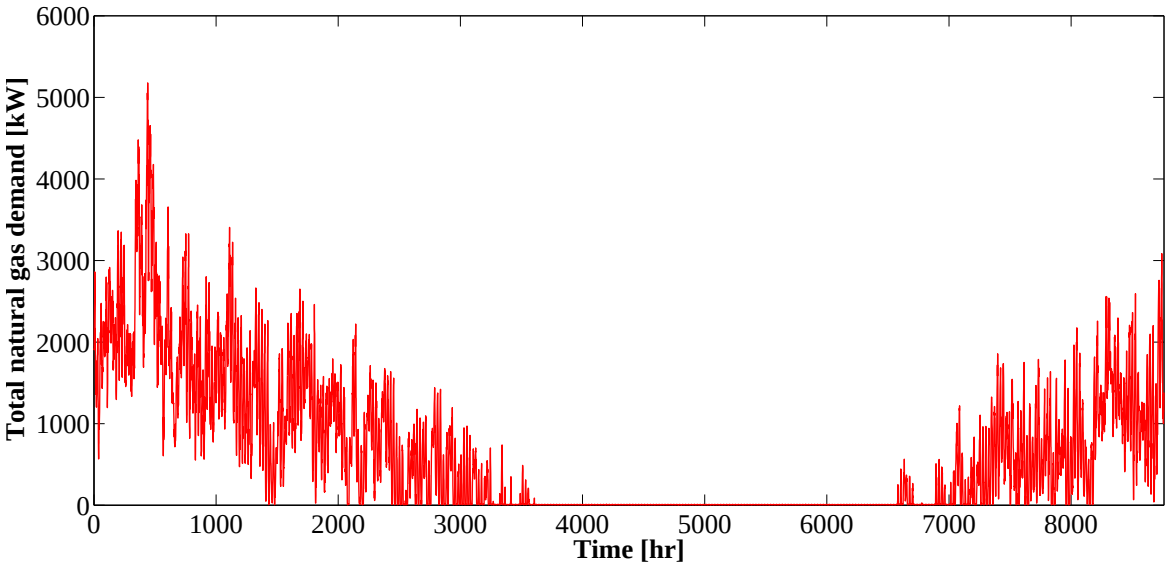

(b)

Fig. 4. Total (a) electricity and (b) natural gas demand of system.

✓Case 3: EGPS method without utilizing electrical storage.

6. Simulation results and discussion

By applying the EGPS method to the described system in the previous section, the following results are obtained. Table 2 lists the energy cost and standard deviation (SD) of electrical and natural gas demands of the three case studies and compares them with the base

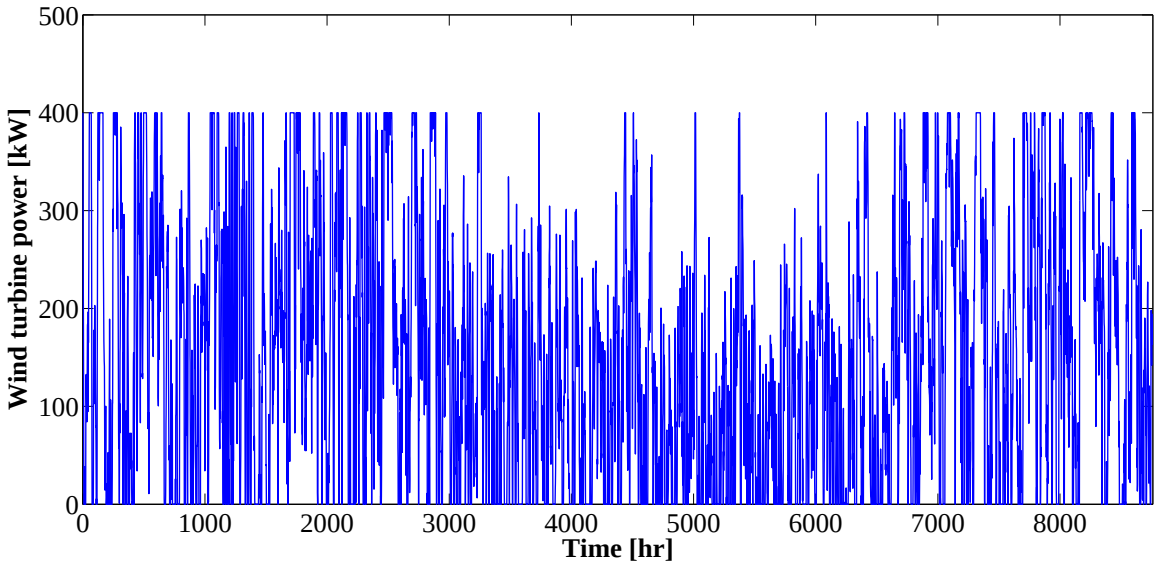

Fig. 5. Electrical power generated by wind turbine.

case and the case without using EGPS method at all. Using EGPS method reduces cost by 16.92% and enhances electricity and natural gas SDs by 8.34% and 66.64%, respectively. As it can be observed, adding P2G unit to the system increases energy costs. However, it has a lot of positive effects on smoothing both electricity and natural gas demand profiles. Similarly, although adding CHP to the system increases energy costs, it has positive impacts on smoothing electricity and mainly natural gas demand profiles. On the other hand, electric storage decreases energy cost while increasing SD of electricity and decreasing SD of natural gas demand. For further inspection, effect of adding each of these devices on the system is given in Table 3 in percent. Decreasing electricity and natural gas profile SDs by 9.29% and 8.29%, respectively, P2G has the highest impact on smoothing both electricity and natural gas demand profiles while the electrical storage has the highest impact on decreasing energy costs of the system with 11.29% impact on cost reduction. This also could be interpreted in a different way. For areas with lower capacity in both electrical and natural gas generation or lines, it is more efficient to use P2G units. For regions with lower capacity in only electrical

generation or lines, using CHP units is more feasible. For areas with financial budget limitations using electrical storages is more beneficial.

Table 2: Result comparison of case studies.

Case name	Energy cost [$]	Electricity SD [kW]	Natural gas SD [kW]
Without EGPS	524063.89	180.85	2662.46
Base case	435403.5	165.76	888.16
Case 1	412671.4	182.73	968.48
Case 2	422696.1	166.65	940.91
Case 3	490821.9	130.09	899.81

Table 3: P2G, CHP and electrical storage effects on results.

Device	Decrease in energy cost [%]	Decrease in electricity SD [%]	Decrease in natural gas SD [%]
P2G	-5.51	9.29	8.29
CHP	-3.01	0.53	5.61
Electrical storage	11.29	-27.42	1.29

Fig. 6a and Fig. 6b illustrate the electricity and natural gas demand profiles after applying EGPS method, respectively. By comparing these figures with Figs. 4a and 4b, it becomes evident that the current EGPS method is successful in shaving peaks and smoothing the demand profiles. By taking advantage of the seasonal load variations and devices like P2G and CHP, the EGPS method is able to use P2G for natural gas production in high natural gas demand times which coincides with lower electricity demand period. On the other hand, CHP was able to fill natural gas demand profile valleys by using natural gas in these hours and producing electricity. This also coincides with peak electricity consumption period.

Methane and direct hydrogen injection by P2G is depicted in Figs. 7a and 7b, respectively. As it can be seen, P2G produces methane and hydrogen mostly in high natural gas demand hours. By doing so, it is able to smooth both electricity and natural gas profiles with using electricity in low electricity demand hours and producing natural gas in high natural gas

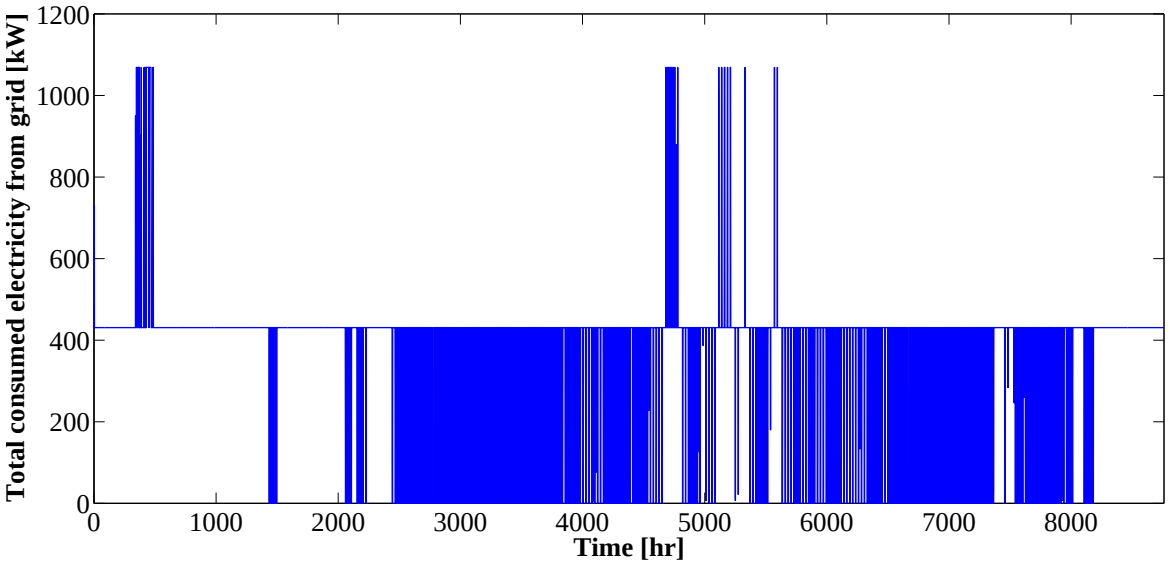

(a)

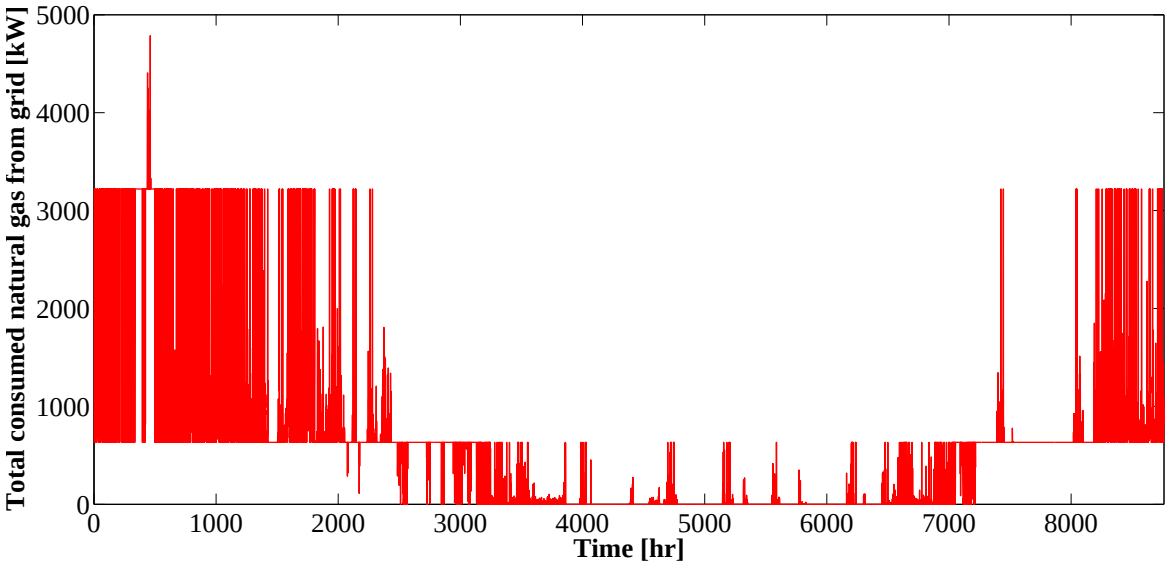

(b)

Fig. 6. Total (a) electricity and (b) natural gas demand of system with EGPS method

periods. Charging and discharging power of the hydrogen storage is shown in Fig. 8 and it is seen that the storage is also only used in peak natural gas demand periods which happens in colder seasons. Charging and discharging are shown by positive and negative values, respectively.

The natural gas consumption by all CHP and gas boiler units is illustrated in Figs. 9 and 10, respectively. As it can be observed, CHP is mostly used during low natural gas demand

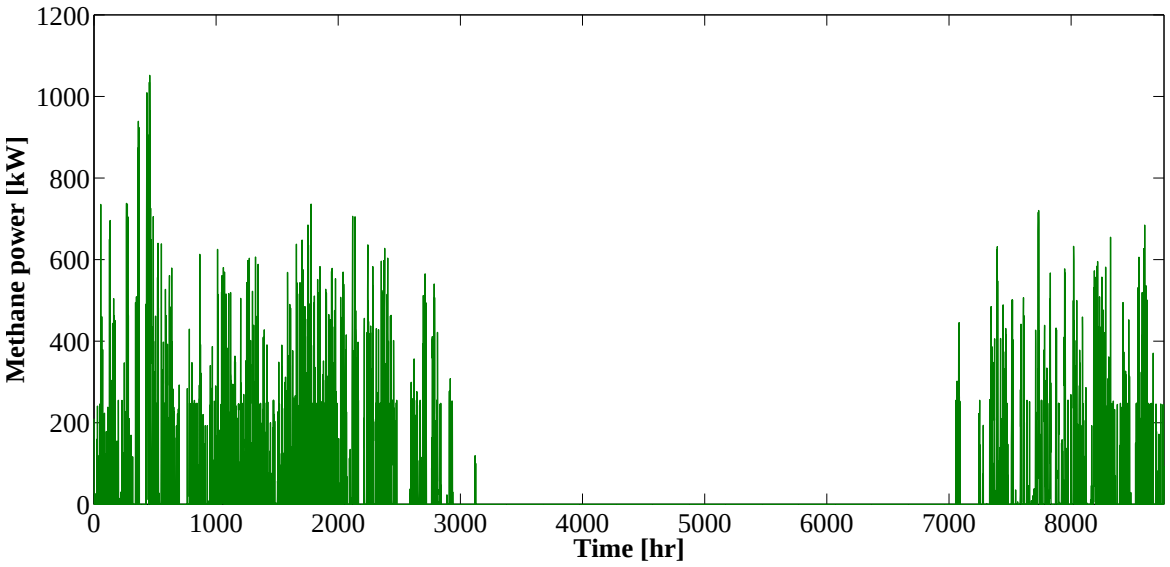

(a)

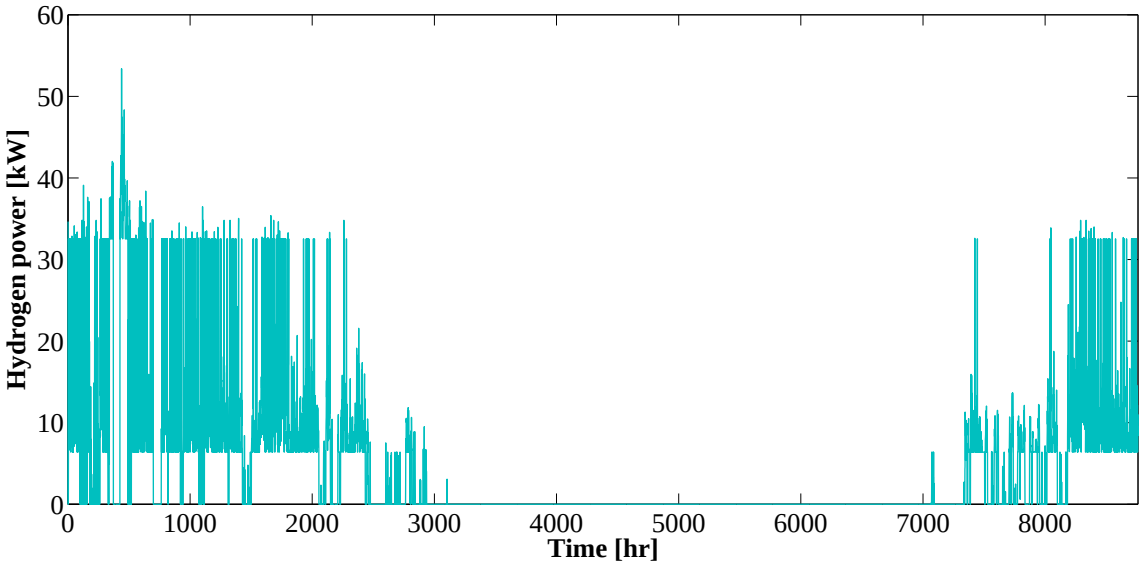

(b)

Fig. 7. Total (a) methane and (b) hydrogen injected to the system by P2G unit.

period to help fill natural gas profile valleys and shave electricity demand peaks by producing electricity. On the other hand, the gas boiler is mostly used in peak period of natural gas demand due to its higher efficiency in providing loads compared to CHP.

The electricity input of all transformers is presented in Fig. 11. Results demonstrate that system transformers work constantly during the whole year. Figs. 12 and 13 show charging and discharging power of the electrical and thermal storages, respectively. Although

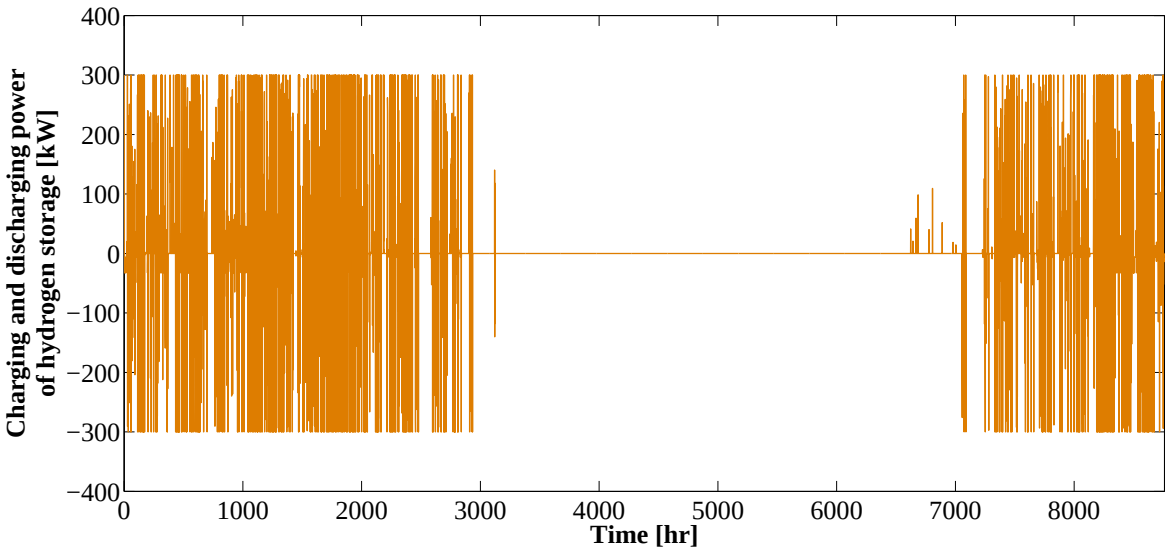

Fig. 8. Charging and discharging power of hydrogen storage inside P2G.

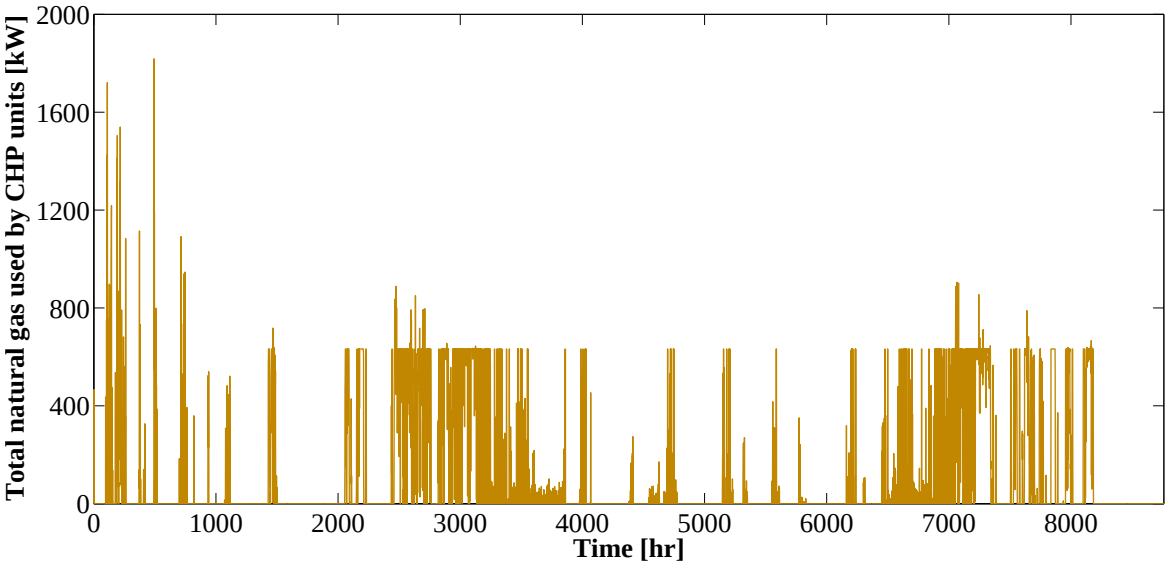

Fig. 9. Natural gas consumption of all CHP units.

electrical storage is used during the whole year, the thermal storage is mostly used during high natural gas demand periods which happens in colder seasons. The average electrical energy exchange among hubs is given in Table 4. The possibility of electricity exchange between hubs, enables better utilization of the devices like CHP which inevitably generate two types of energy, namely electricity and thermal energy, at the output by using natural gas. This

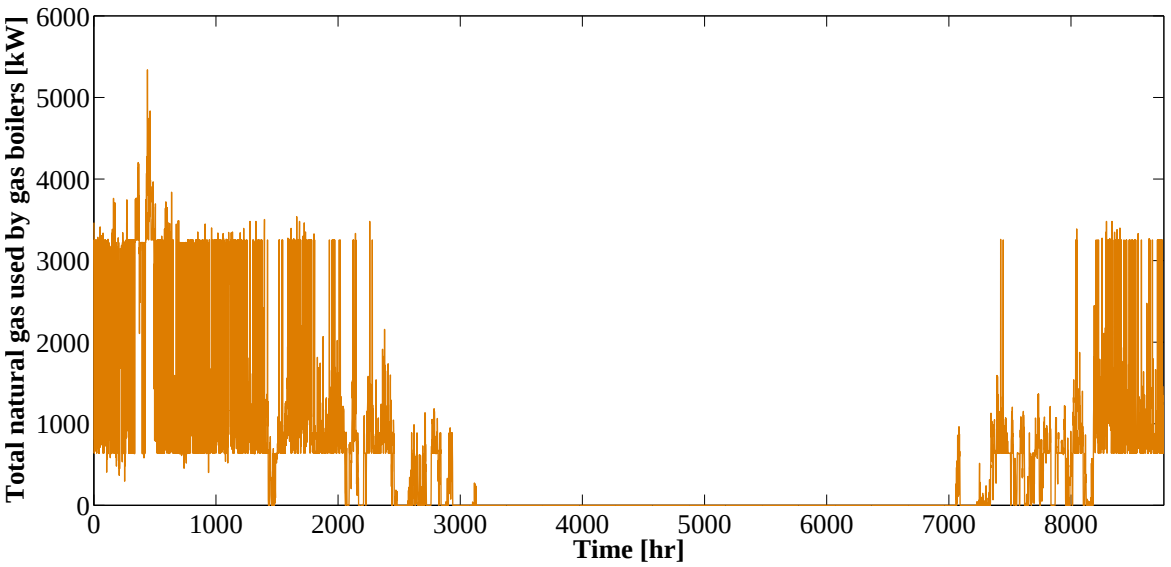

Fig. 10. Natural gas consumption of all gas boiler units.

way, the generated excess electricity can be transmitted to other energy hubs for fulfilling their loads.

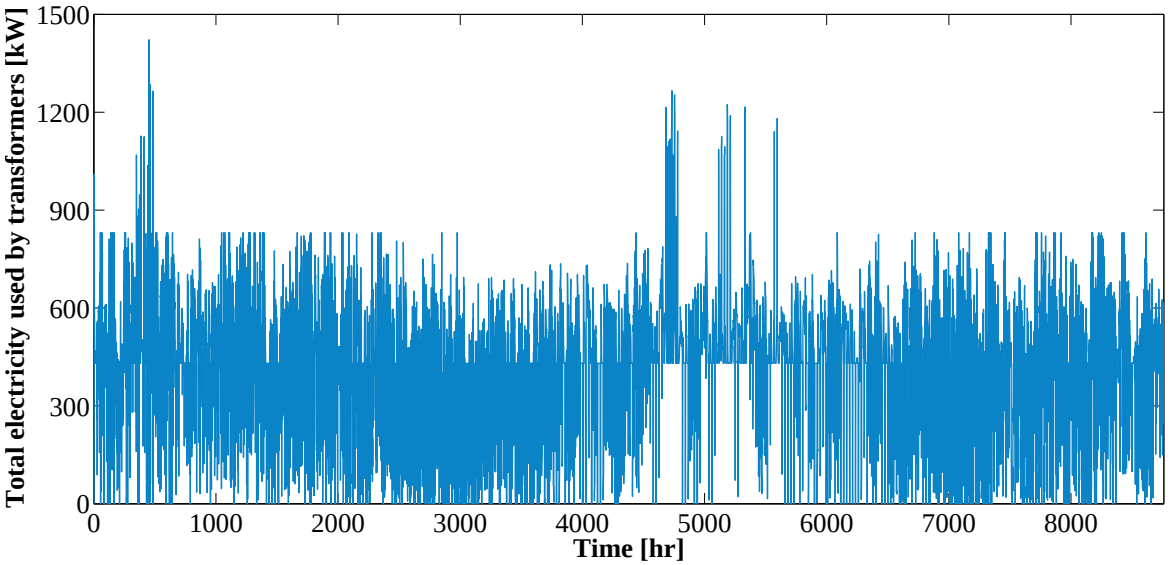

Fig. 11. Electricity input of all transformer units.

Sensitivity analysis are performed for penalty price values by changing the smoothness coefficient. The energy cost and demand profile SD sensitivities to smoothness coefficient

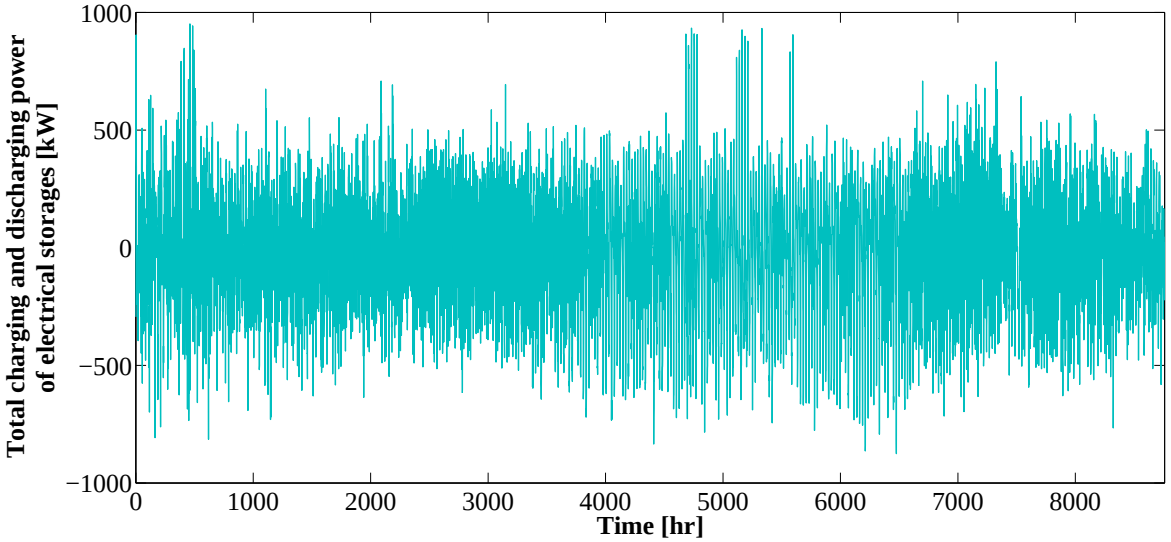

Fig. 12. Charging and discharging power of electrical storages of the system.

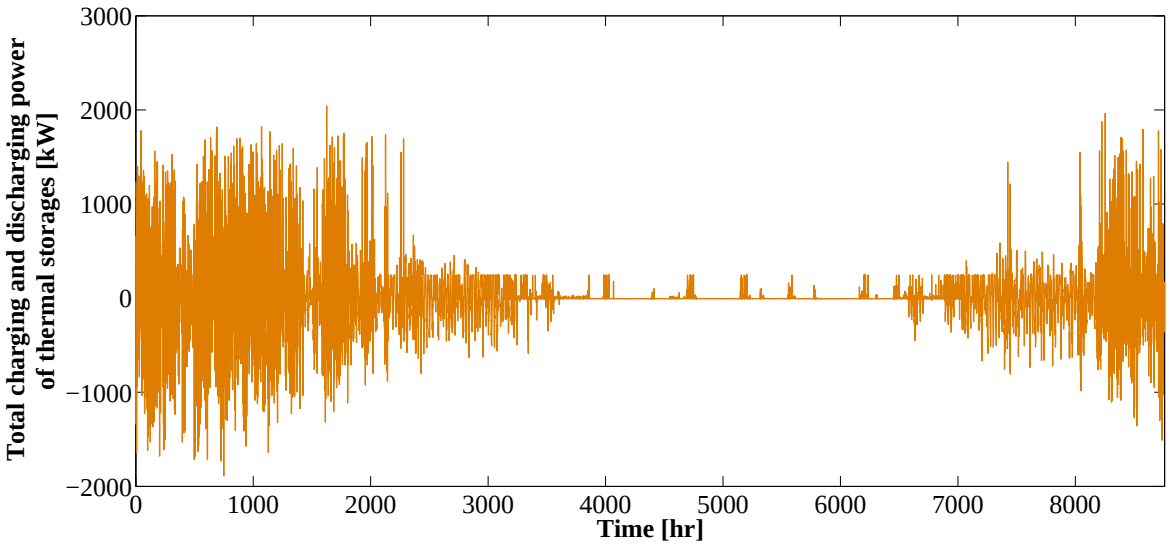

Fig. 13. Charging and discharging power of thermal storages of the system.

are shown in Figs. 14a and 14b, respectively. With the increase in smoothness coefficient, the total energy cost constantly increases until a point. However, the electricity and natural gas demand SDs decrease at the same time. As it can be observed, electricity demand profile has higher flexibility to become smoother compared to the natural gas profile. This is because electricity profile has lower SD in its nature from the beginning. By increasing the

Table 4: Average electrical energy exchange among hubs [kWh].

Line Name	Exchanged energy	Line Name	Exchanged energy	Line Name	Exchanged energy
$P^{ex}_{1,2}$	16.34	$P^{ex}_{3,6}$	1.54	$P^{ex}_{6,4}$	5.01
$P^{ex}_{1,3}$	2.13	$P^{ex}_{4,1}$	3.51	$P^{ex}_{6,5}$	1.38
$P^{ex}_{1,4}$	1.70	$P^{ex}_{4,2}$	3.31	$P^{ex}_{7,8}$	13.68
$P^{ex}_{1,5}$	1.46	$P^{ex}_{4,3}$	0.84	$P^{ex}_{7,9}$	2.10
$P^{ex}_{1,6}$	0.77	$P^{ex}_{4,5}$	25.98	$P^{ex}_{7,10}$	1.50
$P^{ex}_{2,1}$	1.16	$P^{ex}_{4,6}$	1.80	$P^{ex}_{8,7}$	1.56
$P^{ex}_{2,3}$	24.02	$P^{ex}_{5,1}$	4.32	$P^{ex}_{8,9}$	15.98
$P^{ex}_{2,4}$	2.43	$P^{ex}_{5,2}$	3.77	$P^{ex}_{8,10}$	1.76
$P^{ex}_{2,5}$	1.88	$P^{ex}_{5,3}$	3.17	$P^{ex}_{9,7}$	4.84
$P^{ex}_{2,6}$	1.41	$P^{ex}_{5,4}$	0.88	$P^{ex}_{9,8}$	1.68
$P^{ex}_{3,1}$	3.51	$P^{ex}_{5,6}$	18.42	$P^{ex}_{9,10}$	12.77
$P^{ex}_{3,2}$	0.95	$P^{ex}_{6,1}$	6.84	$P^{ex}_{10,7}$	7.17
$P^{ex}_{3,4}$	27.36	$P^{ex}_{6,2}$	6.03	$P^{ex}_{10,8}$	4.98
$P^{ex}_{3,5}$	2.57	$P^{ex}_{6,3}$	5.49	$P^{ex}_{10,9}$	1.53

smoothness coefficient, system reaches the maximum possible smoothness in both electricity and natural gas profiles.

Table 5 compares the individual flexibility of the electricity and natural gas profiles to reach smoothness. The first column represents the energy cost, electricity and gas profile SDs when no penalty factor is considered for natural gas demand variance. On the other hand, the second column shows the same results when penalty factor for electricity demand variance is not taken into account. According to this table, smoothing only electricity profile has adverse effect on natural gas profile smoothness. In the same manner, by smoothing only natural gas profile, electricity profile SD rises. This also shows the importance of studying both demand profiles at the same time. According to the results, the maximum reduction in SD that each of electricity and natural gas profiles can independently achieve is 17.49% and

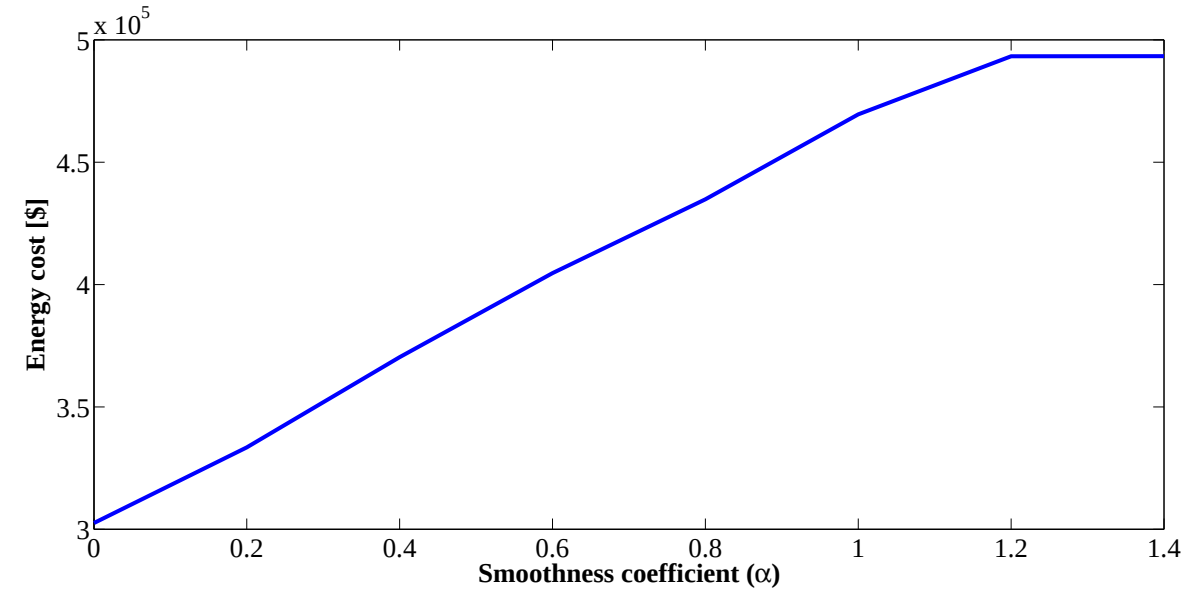

(a)

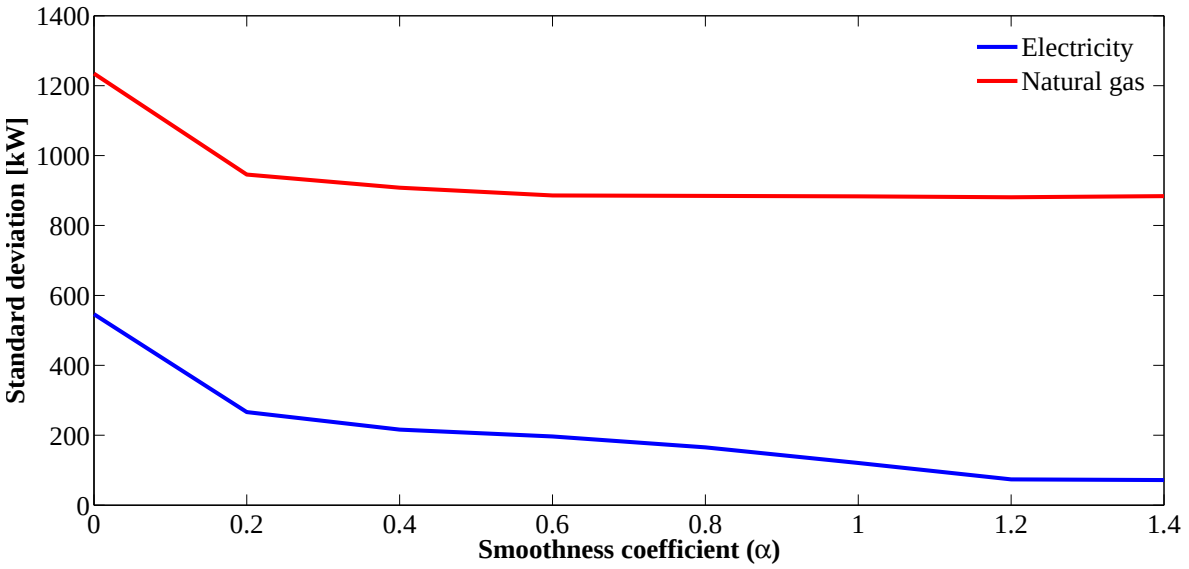

(b)

Fig. 14. Sensitivity of (a) energy cost (b) electricity and natural gas profile SDs to smoothness coefficient.

360 74.36%, respectively compared to the condition when EGPS method is not applied.

361

Table 5: Results of smoothing electricity and natural gas profiles individually.

	$\pi^{gp} = 0$	$\pi^{ep} = 0$	**Base case**
Energy cost [$]	418809.8	418737.9	435403.5
Electricity SD [kW]	149.21	761.40	165.76
Natural gas SD [kW]	1222.80	682.65	888.16

7. Conclusion

The stress on electricity and natural gas networks for supplying demands in the peak consumption period can lead to multiple electrical and natural gas load shedding throughout the year. To address this issue, a new energy management framework named EGPS was proposed in this paper to simultaneously smoothen electricity and natural gas demand profiles. Since natural gas profile valleys coincide with the peak of electricity demand during a year, it was found that the natural gas could be utilized in these periods by devices like CHP technology to fill natural gas valleys as well as shave electricity profile peaks. On the other hand, the peak of the natural gas usage coincides with electricity profile valleys and P2G technology could be used to smoothen both profiles in these periods. The results showed that the EGPS method was able to reduce energy costs by 16.92%. Moreover, it was revealed that 8.34% and 66.64% reduction in electricity and natural gas demand SDs was possible, respectively, after the EGPS application. From the numerical results, it is concluded that among different equipments, P2G had the maximum effect on simultaneous profile smoothing by decreasing electricity and natural gas SDs down to 9.29% and 8.29%, respectively. Furthermore, CHP and electrical storage mostly had positive impacts on gas profile smoothing and energy cost savings, respectively. By employing the proposed method, the system was able to confine the peak of electricity and gas demand and reach a tradeoff between energy saving and profile smoothing which can prevent leveraging of power plants for supplying peak load.

Future studies should focus on other demand side opportunities that increase interdependency between electricity and gas networks and can be used to further smoothen electricity and natural gas demand profiles. Also, the possibility and effects of thermal energy exchange between energy hubs should be studied.

References

[1] Ma, T., Wu, J., Hao, L.. Energy flow modeling and optimal operation analysis of the micro energy grid based on energy hub. Energy Conversion and Management 2017;133:292–306.

[2] Vahid-Pakdel, M., Nojavan, S., Mohammadi-ivatloo, B., Zare, K.. Stochastic optimization of energy hub operation with consideration of thermal energy market and demand response. Energy Conversion and Management 2017;145:117–128.

[3] Ma, M., Ma, X., Cai, W., Cai, W.. Carbon-dioxide mitigation in the residential building sector: A household scale-based assessment. Energy Conversion and Management 2020;.

[4] Ancona, M., Antonucci, V., Branchini, L., Catena, F., Pascale, A.D., Blasi, A.D., et al. Thermal integration of a high-temperature co-electrolyzer and experimental methanator for power-to-gas energy storage system. Energy Conversion and Management 2019;186:140–155.

[5] Budny, C., Madlener, R., Hilgers, C.. Economic feasibility of pipe storage and underground reservoir storage options for power-to-gas load balancing. Energy Conversion and Management 2015;102:258–266.

[6] Maroufmashat, A., Fowler, M., Khavas, S.S., Elkamel, A., Roshandel, R., Hajimiragha, A.. Mixed integer linear programing based approach for optimal planning and operation of a smart urban energy network to support the hydrogen economy. International Journal of Hydrogen Energy 2016;41(19):7700–7716.

406 [7] Chen, S., Wei, Z., Sun, G., Cheung, K.W., Sun, Y.. Multi-linear probabilistic energy
407 flow analysis of integrated electrical and natural-gas systems. IEEE Transactions on
408 Power Systems 2017;32(3):1970–1979.

409 [8] Ni, L., Feng, C., Wen, F., Salam, A.. Optimal power flow of multiple energy carriers
410 with multiple kinds of energy storage. 2016 IEEE Power and Energy Society General
411 Meeting (PESGM) 2016;:1–5.

412 [9] Walker, S.B., Mukherjee, U., Fowler, M., Elkamel, A.. Benchmarking and selection
413 of power-to-gas utilizing electrolytic hydrogen as an energy storage alternative. Inter-
414 national Journal of Hydrogen Energy 2016;41(19):7717–7731.

415 [10] AlRafea, K., Fowler, M., Elkamel, A., Hajimiragha, A.. Integration of renew-
416 able energy sources into combined cycle power plants through electrolysis generated
417 hydrogen in a new designed energy hub. International Journal of Hydrogen Energy
418 2016;41(38):16718–16728.

419 [11] Gholizadeh, N., Vahid-Pakdel, M., Mohammadi-ivatloo, B.. Enhancement of demand
420 supply's security using power to gas technology in networked energy hubs. International
421 Journal of Electrical Power & Energy Systems 2019;109:83–94.

422 [12] Antenucci, A., Sansavini, G.. Extensive CO2 recycling in power systems via power-to-
423 gas and network storage. Renewable and Sustainable Energy Reviews 2019;100:33–43.

424 [13] Qu, K., Zheng, B., Yu, T., Li, H.. Convex decoupled-synergetic strategies for robust
425 multi-objective power and gas flow considering power to gas. Energy 2019;168:753–
426 771.

[14] He, C., Wu, L., Liu, T., Wei, W., Wang, C.. Co-optimization scheduling of interdependent power and gas systems with electricity and gas uncertainties. Energy 2018;159:1003–1015.

[15] Guandalini, G., Campanari, S., Romano, M.C.. Power-to-gas plants and gas turbines for improved wind energy dispatchability: Energy and economic assessment. Applied Energy 2015;147:117–130.

[16] Schiebahn, S., Grube, T., Robinius, M., Tietze, V., Kumar, B., Stolten, D.. Power to gas: Technological overview, systems analysis and economic assessment for a case study in germany. International Journal of Hydrogen Energy 2015;40(12):4285–4294.

[17] Vandewalle, J., Bruninx, K., D'haeseleer, W.. Effects of large-scale power to gas conversion on the power, gas and carbon sectors and their interactions. Energy Conversion and Management 2015;94:28–39.

[18] Nazari-Heris, M., Mohammadi-Ivatloo, B., Gharehpetian, G.. A comprehensive review of heuristic optimization algorithms for optimal combined heat and power dispatch from economic and environmental perspectives. Renewable and Sustainable Energy Reviews 2018;81:2128–2143.

[19] Roshandel, R., Golzar, F., Astaneh, M.. Technical, economic and environmental optimization of combined heat and power systems based on solid oxide fuel cell for a greenhouse case study. Energy Conversion and Management 2018;164:144–156.

[20] Amirante, R., Tamburrano, P.. Novel, cost-effective configurations of combined power plants for small-scale cogeneration from biomass: Feasibility study and performance optimization. Energy Conversion and Management 2015;97:111–120.

[21] Lorestani, A., Gharehpetian, G., Nazari, M.H.. Optimal sizing and techno-economic analysis of energy- and cost-efficient standalone multi-carrier microgrid. Energy 2019;178:751–764.

[22] Hawkes, A., Leach, M.. Solid oxide fuel cell systems for residential micro-combined heat and power in the UK: Key economic drivers. Journal of Power Sources 2005;149:72–83.

[23] Firouzmakan, P., Hooshmand, R.A., Bornapour, M., Khodabakhshian, A.. A comprehensive stochastic energy management system of micro-CHP units, renewable energy sources and storage systems in microgrids considering demand response programs. Renewable and Sustainable Energy Reviews 2019;108:355–368.

[24] Gliński, M., Bojesen, C., Rybiński, W., Bykuć, S.. Modelling of the biomass mCHP unit for power peak shaving in the local electrical grid. Energies 2019;12(3).

[25] Zuo, H., Liu, G., E, J., Zuo, W., Wei, K., Hu, W., et al. Catastrophic analysis on the stability of a large dish solar thermal power generation system with wind-induced vibration. Solar Energy 2019;183:40–49.

[26] E, J., Zhao, X., Qiu, L., Wei, K., Zhang, Z., Deng, Y., et al. Experimental investigation on performance and economy characteristics of a diesel engine with variable nozzle turbocharger and its application in urban bus. Energy Conversion and Management 2019;193:149–161.

[27] E, J., Liu, G., Zhang, Z., Han, D., Chen, J., Wei, K., et al. Effect analysis on cold starting performance enhancement of a diesel engine fueled with biodiesel fuel based on an improved thermodynamic model. Applied Energy 2019;243:321–335.

[28] Reihani, E., Motalleb, M., Ghorbani, R., Saoud, L.S.. Load peak shaving and power smoothing of a distribution grid with high renewable energy penetration. Renewable Energy 2016;86:1372–1379.

[29] Nafisi, H., Abyaneh, H.A., Abedi, M.. Energy loss minimization using PHEVs as distributed active and reactive power resources: a convex quadratic local optimal solution. International Transactions on Electrical Energy Systems 2016;26(6):1287–1302.

[30] Monfared, H.J., Ghasemi, A., Loni, A., Marzband, M.. A hybrid price-based demand response program for the residential micro-grid. Energy 2019;185:274–285.

[31] Cheng, C., Su, C., Wang, P., Shen, J., Lu, J., Wu, X.. An MILP-based model for short-term peak shaving operation of pumped-storage hydropower plants serving multiple power grids. Energy 2018;163:722–733.

[32] Nafisi, H., Agah, S.M.M., Askarian Abyaneh, H., Abedi, M.. Two-stage optimization method for energy loss minimization in microgrid based on smart power management scheme of PHEVs. IEEE Transactions on Smart Grid 2016;7(3):1268–1276.

[33] Uddin, M., Romlie, M.F., Abdullah, M.F., Halim, S.A., Bakar, A.H.A., Kwang, T.C.. A review on peak load shaving strategies. Renewable and Sustainable Energy Reviews 2018;82:3323–3332.

[34] Dréau, J.L., Heiselberg, P.. Energy flexibility of residential buildings using short term heat storage in the thermal mass. Energy 2016;111:991–1002.

[35] Thieblemont, H., Haghighat, F., Moreau, A., Bastani, A., Kuznik, F.. Alternative

method to integrate electrically heated floor in TRNSYS: Load management. CLIMA 2016-proceedings of the 12th REHVA World Congress 2016;.

[36] Barrio, M., Font, J., López, D., Muntasell, J., Tamarit, J.. Floor radiant system with heat storage by a solid-solid phase transition material. Solar Energy Materials and Solar Cells 1992;27(2):127–133. Special Issue on Heat Storage Materials.

[37] Sun, Y., Panchabikesan, K., Joybari, M.M., Olsthoorn, D., Moreau, A., Robichaud, M., et al. Enhancement in peak shifting and shaving potential of electrically heated floor residential buildings using heat extraction system. Journal of Energy Storage 2018;18:435–446.

[38] Zhang, B., E, J., Gong, J., Yuan, W., Zuo, W., Li, Y., et al. Multidisciplinary design optimization of the diesel particulate filter in the composite regeneration process. Applied Energy 2016;181:14–28.

[39] Zhao, X., E, J., Wu, G., Deng, Y., Han, D., Zhang, B., et al. A review of studies using graphenes in energy conversion, energy storage and heat transfer development. Energy Conversion and Management 2019;184:581–599.

[40] yan Zuo, H., quan Luo, Z., lin Guan, J., wei Wang, Y.. Multidisciplinary design optimization on production scale of underground metal mine. Journal of Central South University 2013;20(5):1332–1340.

[41] Bucher, M.A., Haring, T.W., Bosshard, F., Andersson, G.. Modeling and economic evaluation of Power2Gas technology using energy hub concept. 2015 IEEE Power Energy Society General Meeting 2015;:1–5.

[42] HE, C., LIU, T., WU, L., SHAHIDEHPOUR, M.. Robust coordination of interdependent electricity and natural gas systems in day-ahead scheduling for facilitating volatile renewable generations via power-to-gas technology. Journal of Modern Power Systems and Clean Energy 2017;5(3):375–388.

[43] An, D., Yang, Q., Yu, W., Yang, X., Fu, X., Zhao, W.. Sto2Auc: A stochastic optimal bidding strategy for microgrids. IEEE Internet of Things Journal 2017;4(6):2260–2274.

[44] Gholizadeh, N., Abedi, M., Nafisi, H., Askarian-Abyaneh, H., Marzband, M.. Optimization of day ahead distributed intelligent decision-making for a multi-microgrid system. 2018 Smart Grid Conference (SGC) 2018;:1–6.

[45] Office of Energy Efficiency & Renewable Energy (EERE), Available online: https://openei.org; accessed by October 2013 and April 2019.

[46] Philadelphia Electricity Rates, Available online: https://www.electricitylocal.com; accessed by April 2019.

[47] Philadelphia, PA Natural Gas Rates, Available online: https://naturalgaslocal.com; accessed by April 2019.